



UNIVERSITY OF LEEDS

This is a repository copy of *Electrocoalescence of water drop trains in oil under constant and pulsatile electric fields*.

White Rose Research Online URL for this paper:  
<http://eprints.whiterose.ac.uk/93411/>

Version: Accepted Version

---

**Article:**

Vivacqua, V, Mhatre, S, Ghadiri, M et al. (6 more authors) (2015) Electrocoalescence of water drop trains in oil under constant and pulsatile electric fields. *Chemical Engineering Research and Design*, 104. pp. 658-668. ISSN 0263-8762

<https://doi.org/10.1016/j.cherd.2015.10.006>

---

© 2015, Elsevier. Licensed under the Creative Commons Attribution-NonCommercial-NoDerivatives 4.0 International  
<http://creativecommons.org/licenses/by-nc-nd/4.0/>

**Reuse**

Unless indicated otherwise, fulltext items are protected by copyright with all rights reserved. The copyright exception in section 29 of the Copyright, Designs and Patents Act 1988 allows the making of a single copy solely for the purpose of non-commercial research or private study within the limits of fair dealing. The publisher or other rights-holder may allow further reproduction and re-use of this version - refer to the White Rose Research Online record for this item. Where records identify the publisher as the copyright holder, users can verify any specific terms of use on the publisher's website.

**Takedown**

If you consider content in White Rose Research Online to be in breach of UK law, please notify us by emailing [eprints@whiterose.ac.uk](mailto:eprints@whiterose.ac.uk) including the URL of the record and the reason for the withdrawal request.



[eprints@whiterose.ac.uk](mailto:eprints@whiterose.ac.uk)  
<https://eprints.whiterose.ac.uk/>

# ELECTROCOALESCENCE OF WATER DROP TRAINS IN OIL UNDER CONSTANT AND PULSATILE ELECTRIC FIELDS

V. Vivacqua<sup>a</sup>, S. Mhatre<sup>a</sup>, M. Ghadiri<sup>b\*</sup>, A. M. Abdullah<sup>a</sup>, A. Hassanpour<sup>b</sup>, M. J. Al-Marri<sup>c</sup>, B. Azzopardi<sup>d</sup>, B. Hewakandamby<sup>d</sup>, B. Kermani<sup>e</sup>

<sup>a</sup> *Center for Advanced Materials, Qatar University, Doha 2713, Qatar*

<sup>b</sup> *Institute of Particle Science and Engineering, University of Leeds, Leeds LS2 9JT, UK*

<sup>c</sup> *Gas Processing Center, Qatar University, Doha 2713, Qatar*

<sup>d</sup> *Department of Chemical and Environmental Engineering, University of Nottingham, Nottingham NG7 2RD, UK*

<sup>e</sup> *Keytech, Camberley GU15 2BN, UK*

## Abstract

This study addresses the effectiveness of constant and pulsed DC fields in promoting coalescence of dispersed water drops in an oil-continuous phase. For this purpose, a train of drops of relatively uniform size is injected into a stream of flowing sunflower oil. This stream is then admitted to a coalescing section, where an electric field is applied between a pair of ladder-shape bare electrodes. The capability of this device to enhance coalescence of droplets in a chain is investigated at different field intensities, frequencies and waveforms. The effect of the initial inter-droplet separation distance on the process performance is also addressed under constant DC fields. The dominant coalescence mechanism is found to be due to dipole-dipole interaction at low field strength, whereas electrophoresis becomes predominant at higher field strength. Experiments reveal the existence of an optimal frequency, where the average droplet size enlargement is maximized, especially at low field strengths. The droplet size at the outlet of the coalescer is also found to be dependent on the field waveform.

**Keywords:** Electrocoalescence; Electrostatic de-emulsification; Phase separation; Oil treatment.

\*Corresponding author. Tel.: +44 113 343 2406; Fax: +44 113 343 2384.  
E-mail address: m.ghadiri@leeds.ac.uk

## 1. Introduction

The application of electrostatic fields to destabilize water-in-oil dispersions is found in most refineries and oil fields since Cottrell's dust-collector patent [1] was first employed in the dehydration of crude-oil at the beginning of the 20th century [2]. Over the following years, numerous patented designs have been filed and extensive research has been carried out to improve the basic process and understanding of the electrocoalescence mechanisms, as summarized elsewhere [3-9]. The drive to enhance the electrostatically assisted phase separation stems from (i) the low operating costs associated with this process in comparison to other techniques such as centrifugal methods and heat treatment, and from (ii) its environmentally friendly nature as the need for chemical de-emulsifiers is eliminated or reduced [5]. Despite these advantages, capital costs are still high as conventional electrocoalescers are usually large vessels, with the whole operation requiring considerable residence time, typically 30-40 min [6]. Hence, there is a strong need for process intensification by improving the performance and efficiency of the electrostatic treatment through the optimisation of the coalescer design, electrode configuration and electric field parameters.

With respect to this last aspect, AC, DC, pulsed-DC fields and their combinations have been used to enhance coalescence between water droplets. Each field acts according to different mechanisms in promoting phase separation [3]. In particular, pulsed-DC fields, in conjunction with insulated electrodes, have been proposed for applications involving higher water content to avoid short-circuiting [10]. With this type of fields, the main mechanism for droplet growth is based on the induction of dipoles; however, the process seems to be detrimentally affected by the rapid build-up of charge carriers on the electrode insulation coating [7]. Also, the presence of insulation demotes the coalescence mechanism based on the rapid electrophoretic motion of water droplets that become charged by direct contact with bare electrodes.

The role played by the electric field parameters, namely: strength, frequency and waveform, has also been investigated. Generally, separation efficiency improves with increasing applied field strength, but various drop breakup mechanisms can occur if the strength becomes too high [11]. This behaviour results in the formation of tiny droplets which are difficult to separate. A too high field strength also increases the probability that secondary droplets form during droplet-droplet and droplet-interface coalescence [12, 13].

The work of Brown and Hanson [14] is one of the first studies investigating the effect of the electric field frequency on the coalescence of water droplets in oil at a flat liquid-liquid interface. By applying oscillating fields, they determined an optimum frequency at which the critical field strength, at which coalescence was single-staged (i.e. without formation of secondary droplets) and instantaneous, reached a minimum value. The authors explained their findings suggesting that certain frequencies of oscillations corresponded to the drop natural vibration or cavitation, setting up forced vibrations which facilitated coalescence. In a later study, Bailes and Larkai [10] explored the possibility of applying pulsed DC fields to stable dispersions, whilst using insulated electrodes. They found that pulsating DC fields were more effective than constant DC fields in promoting coalescence, suggesting that, with the latter, more electrical energy is lost due to leakage through droplet chains. According to their interpretation, chains are continuously disrupted in pulsed fields, increasing the rate of collision between droplets. They also showed that an optimum frequency exists at a given field strength, especially at low electric field strengths. The frequency-dependent behaviour in the presence of insulated electrodes has been explained by modelling the emulsion-insulated electrode system as a two-layer capacitor [15-17]. According to this analysis, a too low value of frequency results in a significant time interval where the electric field is zero, due to the rapid migration to the insulation layer of mobile charge carriers contained in the oil [16]. On the other hand, too high frequencies would not allow for sufficient movement of these charge carriers, which are assumed to be responsible for the induced droplet charging and the resulting coulombic attraction [16]. However, the existence of an optimum frequency is still controversial. Galvin [18] suggested that the voltage rise and fall time constants of the power supply circuit were important parameters and the existence of an optimum frequency was due to the limitation of the power supply circuit. According to Lundgaard *et al.* [19], instead, efficient operations can be achieved by using AC voltage with high root mean square (RMS) value and applied frequency above a certain threshold, therefore rejecting the idea of the existence of an optimum value for the applied frequency. Similarly, Lesaint *et al.* [20] obtained improved separation performance by increasing frequency until an upper limit. Recently, Mousavi *et al.* [21] have shown that the formation of secondary droplets during droplet-interface coalescence can be suppressed when the pulsed-DC field has a frequency in the range 1-100 Hz. On the other hand, Zhang *et al.* [22] reported that, in oil emulsions subject to AC voltage with frequency in the kHz region, the dehydration efficiency increased with decreasing frequency, suggesting that this behaviour is due to the smaller shape oscillations of droplets in high frequency electrical fields compared to lower ones.

The dependence of the electrocoalescence behaviour on the field waveform has been investigated in a few studies [19-21, 23, 24], but is not well understood. The efficiency of the AC voltage waveforms in destabilizing the emulsions has been ranked as square>sinusoidal>triangular in some studies [19, 20]. This was explained by considering that, for a given peak value, the RMS of the field is the highest with the square waveform and lowest for the triangular one. Berg *et al.* [23] suggested that AC square waves are the most effective in promoting coalescence, as they ensure an electrostatic pressure equivalent to that obtained with a DC field. In contrast, Mousavi *et al.* [21] have recently reported that pulsed DC triangular and sinusoidal waves are the most effective in suppressing the formation of secondary droplets, whereas square waves performance is less satisfactory. In another study, Ingebrigtsen *et al.* [24] reported no appreciable difference in coalescence efficiency when either sinusoidal or square wave types were applied.

In the light of the above considerations, it appears that the effect of the electric field parameters on the electrocoalescence phenomenon is far from being understood. The overall picture is fragmentary and sometimes contradictory. Some confusion is also generated by the fact that the mechanism is strongly dependent on the presence of insulation and the application of AC or pulsed-DC fields. In particular, only few studies [25, 26] have addressed the electrocoalescence behaviour of multi-droplet systems that are subjected to pulsed DC fields between bare electrodes. However, a systematic analysis of the role played by the waveform has not been carried out. The presence of bare electrodes ensures higher rate of collision between droplets due to electrophoresis and dramatically increases the coalescence rate. Therefore research on this type of systems should receive more attention. Furthermore, the phenomenon should be studied under simplified conditions, while retaining the essential features of the real dehydration process. With respect to droplet-droplet and droplet-interface studies, the next level of sophistication is to observe the droplets behaviour when they are present as a train, as the formation of chains is important in electrocoalescence (Pearce [27]). In this regard, Eow and Ghadiri [24] used a pair of ladder-shape electrodes to set up an electric field parallel to the flow direction of a train of drops, ensuring maximum attractive force between adjacent drops. Another advantage of this design is that the presence of the electrodes does not significantly disturb the hydrodynamics of the continuous phase. In the work reported here, the same electrode design has been used, with the aim to assess the effect of the field strength, frequency and waveform on the coalescence behaviour of a train of droplets under the application of constant and pulsed DC fields between bare electrodes.

## 2. Experimental

Tap water and sunflower oil (from Morrisons, Ltd) were used to form a dispersion of aqueous drops in oil and their properties are reported in Table 1. The experiments were carried out at  $20 \pm 2$  °C. No surfactant was introduced into the oil phase and the interfacial tension between the two phases was equal to 25 mN/m. The procedure by which the properties of the two liquids were obtained is described in [12]. The conductivity of the tap water did not change much during the experiments (with measured variations always less than 5%), while the variation of permittivity was assumed to be negligible, considering that the water permittivity is much higher than the permittivity of oil.

A schematic diagram of the experimental set-up is shown in Figure 1 (a). By means of a syringe pump (Model WPI- SP200IZ), the aqueous phase was pumped through a hypodermic needle into the center of the tube containing the oil flowing from the reservoir. In this way, the flow rate of the aqueous phase could be controlled precisely. Small aqueous droplets (around 0.3 mm in diameter) were formed at the outlet of the needle by the shear-force created by the flowing oil. The internal diameter of the tube at the injection point and that of the needle (26G) were 4 mm and 0.26 mm, respectively. The flow of the oil phase to the electrocoalescer was essentially driven by gravity, with the head of liquid in the reservoir kept constant.

The dispersion then flowed from the outlet of the coalescer into a separation unit, where clarification of the oil was achieved by means of gravity settling. The clean oil was then recirculated to the reservoir. The flow rates of the aqueous and sunflower oil phases were  $1 \mu\text{l min}^{-1}$  and  $0.18 \text{ l min}^{-1}$ , respectively, in all the experiments, except those where the inter-droplet separation distance was wider and the water flowrate was  $0.5 \mu\text{l min}^{-1}$ . The average oil velocity in the coalescer was 6 mm/s and, with the equivalent diameter of the rectangular duct equal to 16.7 mm, this velocity corresponds to a Reynolds number of 1.98. The oil flow was therefore laminar. As for the water phase, in the most conservative scenario where the droplets flowed with the same velocity of the oil, the terminal Reynolds number is equal to 0.04, revealing creeping flow conditions. In these conditions, the shear rate exerted on the droplets is practically negligible.

The electrocoalescer was made up of Perspex to facilitate visualisation of the coalescence process. Figure 1b is a drawing representing the geometry of the electrodes. The separation distance between the two electrodes was 15 mm, while the distance between each horizontal bar in both electrodes was 3 mm. The overall dimension of the grounded electrode was 10 mm x 50 mm. In order to reduce the probability of

short-circuiting due to the formation of a water layer on the base of the coalescer, the high-voltage electrode was truncated at a distance of 10 mm from the Perspex base. This produced some downward preferential flow in the region between the electrodes. Although this phenomenon slightly changed the angle between the electric field and the droplet flow direction in all the experiments, its effect has been considered negligible. Both electrodes were made of polished brass.

The high voltage electrode was connected to a positive polarity high voltage direct current source, while the other electrode was grounded. A specialized high voltage dc and pulsating dc unit (TREK 20/20C), with high slew rate (greater than  $450 \text{ V}/\mu\text{s}$ ) and 7.5 kHz bandwidth (-3dB), was used to apply the electric field with good accuracy at high frequency. Both pulsed and constant dc fields were applied and their effectiveness in enhancing coalescence was assessed.

For this purpose, a digital camera (Photrom Fast Cam SA5) was used to observe the coalescence phenomenon and the diameter of the droplets was measured by means of ImageJ software. In all the experiments, the total time of application of the field was about 20 s, and the measured droplet size at the outlet was obtained by averaging the droplet population downstream the coalescing section. The maximum error associated with measurement of the droplet size by image analysis is estimated to be around 0.03 mm. The number of droplets analysed in each experiment was variable and turned out to depend on the applied voltage. The number of droplets which exit the device during the same time interval decreased with increasing the applied voltage, as the enhancement of coalescence produced fewer and larger drops. Thus, the number of droplets analysed in each experiment varied approximately from 100 to 300, at high and low voltage respectively. The experiments were repeated three times. In some cases, the error bars were calculated considering the error associated with the image analysis, whenever this type of error introduced a greater variability.

Probability density functions (PDFs) were obtained according to the following procedure. The number of bins in which each distribution is discretized was determined by setting the ratio between the average size of consecutive bins equal to the cubic root of 2, which corresponds to the enlargement factor of a pairwise coalescence event. The values of the y axis were then calculated dividing the number of droplets in each bin by the bin size and the total number of droplets in the distribution, so that the area under each distribution is equal to 1.

The droplet size distribution was determined at three different values of the electric field strength (peak value), namely 67, 134 and  $335 \text{ kV m}^{-1}$ . These field intensities correspond to electrocapillary numbers

equal to 0.0025, 0.005 and 0.0125, respectively, when evaluated at the inlet of the device. The electrocapillary number is defined as:

$$Ca_{el} = \frac{E_0^2 d_{in} \epsilon_{oil}}{\gamma}$$

where  $E_0$  is the peak value of the applied field intensity,  $d_{in}$  is the initial droplet size,  $\epsilon_{oil}$  the permittivity of the oil phase and  $\gamma$  the oil/water surface tension. An average inlet droplet size of 0.32 mm was used for this calculation. Frequencies in the range 0.5-100 Hz were explored and the performance of three waveforms were assessed, apart from constant fields. Some examples of oscilloscopes representing the different waveforms applied are reported in Figure 2.

### 3. Results and discussion

#### 3.1 Constant DC fields

The first part of the experimental work presented herein addresses the evaluation of the electrocoalescence performance under the application of constant DC fields. Results are shown for two different conditions: (a) the droplets forming the chain are almost touching, (b) separated by a distance approximately equal to one droplet diameter. The initial average droplet size (about 0.3 mm) was approximately the same in the two cases. Snapshots in Figures 3a & 3b depict the two different situations, respectively. The distance between droplets is an important variable in the coalescer design, as it can be related to the water content in an actual emulsion: varying the inter-droplet separation therefore allows investigating possible different behaviours in the electrocoalescence mechanism between systems with dissimilar water contents.

##### 3.1.1 Coalescence of contiguous droplets

The size distribution of the water droplets subjected to constant DC fields is shown in Figure 4. Probability density functions (PDFs) are reported for the inlet as well as for the outlet at varying applied electric field strength between the electrodes. The average inlet droplet size is about 0.3 mm, whereas the mean outlet diameter increases with the applied voltage. As a first remark, inspection of Figure 4 reveals that the span of the distribution increases with the field intensity. More interestingly, the distribution becomes bi-modal when the electric field is raised to 335 kV m<sup>-1</sup>, as a clear indication of the onset of a different mechanism of coalescence, which leads to the simultaneous presence of large droplets and much smaller ones. In

support of this statement, Figure 5 is presented to compare the observed coalescence behaviour between the two cases, where 134 and 335  $\text{kV m}^{-1}$  electric fields are applied. At 134  $\text{kV m}^{-1}$  (Figure 5a), coalescence occurred only between neighbouring droplets according to the dipole-dipole interaction mechanism. On the other hand, at 335  $\text{kV m}^{-1}$ , droplets acquired a sufficient charge upon contact with the electrodes and started to accelerate rapidly under the influence of the electrophoretic force, as shown by the blur images of droplets circled in red in Figure 5b. Thus, the application of a sufficiently high voltage between the electrodes produces an additional mechanism of “migratory coalescence”, during which rapidly moving charged droplets intercept and coalesce with other droplets along their path.

In Figure 6, the ratio between the average outlet diameter and the mean inlet size  $d_{\text{out}}/d_{\text{in}}$  is plotted as a function of the electric field strength. Error bars are calculated by using the upper and lower values of the average outlet droplet size determined in the three repeated experiments, while keeping the inlet average size constant. As expected, the average droplet enlargement increases as the field strength increases; however, the variability of the measurement at 335  $\text{kV m}^{-1}$  is significantly large, with the size ratio varying approximately from 1.8 to 2.1. This is due to the chaotic electrohydrodynamic flow at high electric fields, which results in a different electrode-drop contact and, in turn, in the different amount of charge acquired by the droplets.

At higher field strengths, short-circuiting occurs, the onset of which was observed above 400  $\text{kV m}^{-1}$  in all the experimental cases, i.e. regardless of the applied frequency, waveform or inter-droplet distance. The electric field threshold for short-circuiting probably corresponds to the condition, where droplets become unstable and disintegrate in many tiny droplets, which can easily bridge the two electrodes. An image of a typical electrostatic discharge at 467  $\text{kV m}^{-1}$  is shown in Figure 7.

### 3.1.2 Coalescence of droplets with wider inter-droplet separation

The inter-droplet distance is about one droplet diameter in this set of experiments. In order to carry out a quantitative comparison with the previous condition, where the droplets in the chain are almost in contact with each other, the ratio  $d_{\text{out}}/d_{\text{in}}$  is plotted as a function of the electric field strength in Figure 8 for both cases. The data reported in this figure reveal that increasing the inter-droplet distance has important consequences on the extent of coalescence achieved. When the distance between the droplets is about one initial droplet diameter, the size ratio  $d_{\text{out}}/d_{\text{in}}$  does not differ significantly from unity for fields lower than 200  $\text{kV m}^{-1}$ . The absence of appreciable coalescence stems from the fact that the separation

between the droplets is probably too large in this case for dipole-dipole interaction to be active due to its short-range nature. These results also suggest that in emulsions with low water content there exists an electric field threshold below which coalescence is likely to occur only to a limited extent, at least, as far as dipole-dipole attraction remains the only mechanism by which coalescence is promoted. However, at higher electric fields, the dominant coalescence mechanism can become electrophoresis: in Figure 8, the data relevant to initially separated droplets reveal a rapid coalescence improvement when the electric field is  $335 \text{ kV m}^{-1}$ , albeit reaching a value of  $d_{\text{out}}/d_{\text{in}}$  which is lower than that measured in the case of contiguous droplets. This is due to the fact that the number of droplets admitted per unit time into the coalescence section of the device is smaller. As a matter of fact, when a droplet moves between the electrodes due to electrophoresis, the likelihood to contact other droplets increases with their concentration. However, these results confirm the transition to the migratory coalescence regime in which a significant amount of charge is transferred to the droplets from the electrodes. In this case, the results become less dependent on the initial inter-droplet distance as dipole-dipole attraction ceases to be the main mechanism for coalescence. By further increasing the electric field to  $400 \text{ kV m}^{-1}$ , the size ratio decreases, as shown in Figure 8. This is due to the fact that when the size of the enlarged coalesced drops exceeds a critical value of the electrical capillary number, they break into fine droplets reducing the average drop size in the system [12, 13]. When the field is further increased above  $400 \text{ kV m}^{-1}$ , short-circuiting of the system occurs as in the previous case.

### 3.2 Pulsatile DC fields

The capability of pulsatile DC fields to enhance coalescence has been assessed by utilising three different waveforms for the applied DC voltage: square (with duty cycle = 0.5), sawtooth and half-sinusoidal waves. Coalescence was investigated in the frequency range between 0.5 – 100 Hz. Contiguous droplets were fed to the coalescer in all these experiments.

#### 3.2.1 Square waves

Probability density functions of inlet and outlet droplet size distributions are shown in Figure 9 for the case where a pulsed DC field is applied with a square waveform. The variation of the population of droplets in terms of their size as a function of some selected values of frequency and maximum nominal field strength,  $E_0$  (peak value), shows that both parameters affect the output of the coalescer. Similar to what was obtained with constant fields, the variance of the distribution becomes larger with an increase in the field intensity and the presence of two peaks at  $335 \text{ kV m}^{-1}$  (Figure 9c) denotes a product comprised of

two main populations of large and comparably small droplets as a result of the onset of the electrophoretic mechanism. The effect of frequency is also significant; a clear optimum value of the applied frequency was observed at relatively low field intensities, namely at 67 and 134  $\text{kV m}^{-1}$  (Figures 9a & 9b, respectively). This optimal value is equal to 1 Hz in both cases. On the other hand, the dependence on frequency is not substantial at 335  $\text{kV m}^{-1}$ . An overall comparison of the data suggests that 1 Hz frequency and 134  $\text{kV/m}$  strength (Figure 9b) are optimum process conditions. The average droplet size is comparable with that of 335  $\text{kV m}^{-1}$  (Figure 9c), but the variance of the outlet droplet size distribution is less wide. In the former case, a better overall transformation as the smallest size cuts are eliminated. For a quantitative comparison in terms of average droplet enlargement, the size ratio  $d_{\text{out}}/d_{\text{in}}$  is reported in Figure 10 for all the conditions investigated using square waves. Dotted lines representing what was achieved with constant fields are also reported in these graphs for further comparison. It is clear that operating the coalescer at the optimum frequency leads to an increase of droplet coalescence at low field strength, i.e. at 67 and 134  $\text{kV m}^{-1}$  (Figures 10a & 10b, respectively). However, at higher field strength of 335  $\text{kV m}^{-1}$  (Figure 10c) the average values of  $d_{\text{out}}/d_{\text{in}}$  fall below that observed with constant DC fields with the same  $E_0$ . The maximum value of  $d_{\text{out}}/d_{\text{in}}$  is around 1.8. If the coalescence sequence is considered to be pairwise, then this size ratio corresponds to about 2.5 times pairwise coalescence. Despite this, it is not possible to conclude that the pulsatile field is less effective than the constant one in this case, as the error bars associated with the measurements at 335  $\text{kV m}^{-1}$  (see also Figure 6) are large. Nonetheless, the role played by frequency is less important at high electric fields, most probably due to the transition from the dipole-dipole interaction regime to the electrophoretic one. Electrophoresis strongly depends on the average field strength, which is higher for constant fields than for square wave fields with the same strength peak value.

### 3.2.2 Sawtooth waves

The probability density functions of inlet and outlet droplet size distributions obtained with sawtooth waves at different field strengths and some selected frequencies are shown in Figure 11. Compared to the previous case, the variance of the distributions is larger at all field strengths, denoting an increase in polydispersity and average droplet size. At 67 and 134  $\text{kV m}^{-1}$  (Figures 11a & 11b) the optimum frequency is 10 and 20 Hz, respectively, with a shift of the optimal value towards higher frequencies in comparison with square waves. A rationale for this may stem from the fact that with square waves the time during which the field is on would be too short at high frequencies. In the light of this interpretation, the ratio between the field on-time and the total time (i.e the duty cycle) can be an important variable while using

square waves. However, these results provide confirmation of the existence of an optimum frequency at low field strengths also with this wave type, whereas at  $335 \text{ kV m}^{-1}$  the dependence on frequency is less certain. In Figure 12 it is shown that the use of sawtooth waves leads to an improvement of coalescence compared to both constant and square wave-type fields. At 67 and  $134 \text{ kV m}^{-1}$  (Figure 12a & b), the size ratio  $d_{\text{out}}/d_{\text{in}}$  is larger than what was observed with constant fields at all investigated frequencies, whereas this difference is again not important at  $335 \text{ kV m}^{-1}$  (Figure 11c), i.e. when migratory coalescence becomes predominant. Using this type of waves with the maximum value of  $d_{\text{out}}/d_{\text{in}}$  is around 2 (equal to about three times pairwise coalescence).

### 3.2.3 Half-sinusoidal waves

The results obtained by using sinusoidal waves are presented in Figures 13 and 14. Droplet size distributions are somewhat similar to the previous cases at 67, 134 and  $335 \text{ kV m}^{-1}$  (Figures 13a, 13b & 13c, respectively). Furthermore, optimal frequencies of 10-20 Hz were observed as with sawtooth waves.

At 67 and  $134 \text{ kV m}^{-1}$  (Figures 14a & 14b), the coalescence enhancement brought about by sinusoidal and sawtooth waves is comparable, with the latter being slightly more effective, as it can be observed from comparison of Figures 12 and 14. These results are in agreement with what was found previously in another study [21], where waveforms were ranked as sawtooth  $\geq$  half-sinusoidal  $>$  square waves, in terms of coalescence quality, i.e. complete coalescence without generating secondary droplets, for both droplet-droplet and droplet-interface systems. These findings are confirmed in the present study also when a larger population of droplets is involved.

More interestingly, the data in Figure 13 reveal that this type of waves can appreciably enhance coalescence compared to constant field even at  $335 \text{ kV m}^{-1}$  (with a maximum value of  $d_{\text{out}}/d_{\text{in}}$  of approximately 2.5, equivalent to about four times pairwise coalescence), at which electrophoretic effects become predominant. In this regard, it should be noted that a higher average field strength is applied with the sinusoidal waveform, about 30% larger in comparison with square and sawtooth waves.

## 4. Discussion

The theoretical RMS and average values of the electric field for the different waveforms used are reported in Table 2. Previous studies carried out with insulated electrodes [19, 20] have related the effectiveness of the different waveforms to the root mean square (RMS) of the field, which corresponds to the value of a DC voltage giving the same electrical power. According to this interpretation and by inspection of Table 2, square and half-sinusoidal waves should have equal performance and be superior to sawtooth waves. However, this is clearly at odds with the experimental findings presented in the previous section, where half-sinusoidal waves provided better results in terms of droplet growth compared to both square and sawtooth waves, especially at high field strength. In this regard, the values listed in Table 2 reveal that the half-sinusoidal waves are endowed with the highest value of the average field intensity. Thus, half-sinusoidal waves may be more effective at high field strengths, compared to the other waveforms, as the charge transferred from the conductive electrodes is directly proportional to the field intensity [7]. However, the value of the average field strength cannot be the only criterion of interpretation of the experiments, as this would imply that the best performance are obtained using constant fields, a conclusion which is proved erroneous by experimental evidence. Therefore the role played by the operating frequency is as important as the field strength, and both variables must be tuned to optimize the process. On the other hand, a too high field, although below the short-circuiting threshold, can promote formation of large drops by electrophoresis accompanied by a significant number of small droplets, which do not undergo coalescence, thus reducing the efficiency of the overall process.

At lower field intensities, modulating the field frequency is an important tool to optimise the process performance with all waveforms. Among them, square waves have proved to provide less satisfactory results, probably because the duty cycle can be an additional important parameter with this type of waveform. Models which attempt to explain the existence of an optimum frequency are available [15-17] but only for insulated electrodes. For bare electrodes the effect of frequency on coalescence is more uncertain. Oscillating droplet deformation caused by a pulsatile field can probably weaken the film resistance between neighbouring droplets. It could also influence the migration of surfactants and impurities over the surfaces, causing interfacial tension gradients, both cases facilitating coalescence. It should also be noted that once two droplets are in direct contact with each other and the film separating them has been broken, continued exposure to electrical field is not required to achieve or improve coalescence of the same two droplets. However, when considering the two droplets as part of a larger dispersion or emulsion, continued electrostatic exposure will obviously have an effect since it will increase the likelihood of further coalescence of the merged droplet with other neighbouring droplets. Hence we consider pulsatile fields to be the most appropriate type for this application.

## **5. Conclusions**

The effect of the field strength, frequency and waveform on the coalescence process of a chain of droplets between bare electrodes has been investigated. The main coalescence mechanism is found to be dipole-dipole interaction at low field strengths, whereas migratory coalescence, due to electrophoresis, becomes predominant at higher intensities. However, coalescence can occur only after the onset of the electrophoretic regime when the initial inter-droplet distance is wide.

The optimum frequency for coalescence with each waveform has clearly been determined, especially at low field intensities. By properly tuning the operating frequency, coalescence under pulsed-DC-fields can be significantly improved compared to constant fields.

Varying the electric field waveform can appreciably affect the rate of electrocoalescence. The half-sinusoidal waveform is found to be the most effective in promoting coalescence, especially in the electrophoretic regime. The square waveform has in contrast provided the least satisfactory results; assessing the effect of the duty cycle on the process performance should be the subject of further study. Another short-term objective can be the assessment of the effect of different waveforms with the same RMS value of the applied field. Finally, an important subject for future work is to study the effect of the oil conductivity, as varying the relaxation time can strongly affect the efficiency of the electrophoretic mechanism.

## **Acknowledgements**

This work was made possible by NPRP grant #5-366-2-143 from the Qatar National Research Fund (A Member of The Qatar Foundation). The statements made herein are solely the responsibility of the authors.

The assistance of Messrs Robert Harris and Matthew Buckley in setting up the experimental rig is gratefully acknowledged.

A. M. Abdullah is on leave from Chemistry Department, Cairo University, Giza, Egypt.

## References

1. Cottrell, F. G., 1908. Art of separating suspended particles from gaseous bodies. US Patent No 895 729.
2. Cottrell, F. G., 1911. Process for separating and collecting particles of one liquid suspended in another liquid. US Patent No 987 114.
3. Taylor, S.E., 1996. Theory and practice of electrically enhanced phase separation of water-in-oil emulsions. *Trans. IChemE* 74, (A), 526–540.
4. Eow, J.S., Ghadiri, M., Sharif, A.O. and Williams, T., 2001. Electrostatic enhancement of coalescence of water droplets in oil: a review of the current understanding. *Chem Eng J*, 84 (3), 173–192.
5. Eow, J.S. and Ghadiri, M., 2002. Electrostatic enhancement of coalescence of water droplets in oil: a review of the technology. *Chem Eng J*, 85 (2–3), 357–368.
6. Urdahl, O., Wayth, N. J, Førdedal, H., Williams, T. J., Bailey, A. G. Compact Electrostatic Coalescer Technology, In: Sjöblom, J. (Ed.), *Encyclopedic Handbook of Emulsion Technology*, Marcel Dekker, 2001.
7. Lundgaard, L. E., Berg, G., Ingebrigtsen, S. and Atten, P. Fundamental aspects of electrocoalescence. In: J. Sjöblom (Ed.), *Emulsions and Emulsion Stability*, 2nd edition, Marcel Dekker, 2006.
8. Less, S. and Vilagines, R., 2012. The electrocoalescers technology: Advances, strengths and limitations for crude oil separation. *J Petrol Sci Eng*, 81, 57–63.
9. Mhatre, S., Vivacqua, V., Ghadiri, M., Abdullah, A.M., Al-Marri, M.J., Hassanpour, A., Hewakandamby, B., Azzopardi, B., Kermani B., 2015. Electrostatic phase separation: A review. *Chem Eng Res Des*, 96, 177-195.
10. Bailes, P.J., Larkai, S.K.L., 1981. An experimental investigation into the use of high voltage dc fields for liquid phase separation. *Trans IChemE* 59 (4), 229–237.
11. Williams, T.J. and Bailey, A.G., 1986. Changes in the size distribution of a water-in-oil emulsion due to electric field induced coalescence, *IEEE Trans. Ind. Appl.*, 1A–22 (3), 536–541.
12. Mousavichoubeh M., Ghadiri M. and Shariaty-Niassar M., 2011. Electro-coalescence of an aqueous droplet at an oil–water interface, *Chem Eng Process*, 50, 338-344.
13. Mousavichoubeh M., Shariaty-Niassar M. and Ghadiri M., 2011. The effect of interfacial tension on secondary drop formation in electrocoalescence of water droplets in oil, *Chem Eng Sci*, 66, 5330–5337.
14. Brown, A.H. and Hanson, C., 1965. Effect of oscillating electric fields on coalescence in liquid–liquid systems. *Trans Faraday Soc*, 61, 1754–1760.

15. Joos, F.M. and Snaddon, R.W., 1985. On the frequency dependence of electrically enhanced emulsion separation, *Chem Eng Res Des*, 63 (5), 305-311.
16. Bailes P.J., 1995. An electrical model for coalescers that employ pulsed dc fields, *Trans IChemE*, 73 (A), 559-566.
17. Midtgard O-M., 2009. Electrostatic field theory and circuit analysis in the design of coalescers with pulsed dc voltage, *Chem Eng J*, 151, 168-175.
18. Galvin, C.P., 1986. Design principles for electrical coalescers, *IChemE Symp. Ser.* 88, 101–113.
19. Lundgaard, L., Berg, G., Pedersen, A., Nielsen, P.J., 2002. Electrocoalescence of water drop pairs in oil. In: *Proceedings of the 14th International Conference on Dielectric Liquids*, Graz, Austria.
20. Lesaint, C., Glomm, W.R., Lundgaard, L.E., Sjöblom, J., 2009. Dehydration efficiency of AC electrical fields on water-in-model-oil emulsions, *Colloids Surf A: Physicochem Eng Aspects* 352, 63–69.
21. Mousavi, S.H., Ghadiri, M. and Buckley, M., 2014. Electro-coalescence of water drops in oils under pulsatile electric fields. *Chem Eng Sci*, 120, 130 - 142.
22. Zhang, Y., Liu, Y. and Ji, R., 2011. Dehydration efficiency of high-frequency pulsed DC electrical fields on water-in-oil emulsion, *Colloids Surf. A: Physicochem. Eng. Aspects*, 373, 130–137.
23. Berg, G., Lundgaard, L.E., Becidan, M. and Sigmond, R.S., 2002. Instability of electrically stressed water droplets in oil. In: *Proceedings of the 14th International Conference on Dielectric Liquids*, Graz, Austria.
24. Ingebrigtsen, S., Berg, G. and Lundgaard, L.E., 2005. Electrocoalescence in stagnant emulsions dielectric liquids. In: *IEEE International Conference*.
25. Eow, J. S., and Ghadiri, M., 2003. Drop/drop coalescence in an electric field: the effects of applied electric field and electrode geometry, *Colloids and Surfaces A: Physicochem. Eng. Aspects*, 219, 253-279.
26. Eow, J. S., Ghadiri, M. and Sharif A.O., 2002. Electrostatic and hydrodynamic separation of aqueous drops in a flowing viscous oil. *Chem Eng Process*, 41, 649–657.
27. Pearce C. A. R., 1953. The mechanism of the resolution of water-in-oil emulsions by electrical treatment. *Br J Appl Phys*, 5, 136–143.

## Captions

**Figure 1:** Experimental rig and electrode design.

**Figure 2.** Waveforms generated by the high voltage unit: (a) sinusoidal waves, (b) sawtooth waves, (c) square waves.

**Figure 3:** Snapshots of the droplet train for the two experimental cases: (a) contiguous and (b) separated droplets.

**Figure 4:** Probability density functions of water droplets size distributions under constant DC fields at varying field intensity.

**Figure 5:** Experimental images revealing different coalescence mechanisms under constant DC fields at: a) 134 and b) 335  $\text{kV m}^{-1}$ .

**Figure 6:** Average droplet enlargement of a train of contiguous droplets under constant electric fields.

**Figure 7:** Electric discharge due to short-circuiting under a constant electric field of 467  $\text{kV m}^{-1}$ .

**Figure 8:** Effect of inter-droplet separation on droplet coalescence under constant electric fields.

**Figure 9:** Probability density functions of inlet and outlet droplet size distributions under square DC fields at varying frequency and field intensity: (a) 67, (b) 134 and (c) 335  $\text{kV m}^{-1}$ .

**Figure 10:** Average droplet enlargement with square DC fields at varying frequency and field intensity: (a) 67, (b) 134 and (c) 335  $\text{kV m}^{-1}$ . Comparison with constant DC fields.

**Figure 11:** Probability density functions of inlet and outlet water droplet size distributions under sawtooth DC fields at varying frequency and field intensity: (a) 67, (b) 134 and (c) 335 kV m<sup>-1</sup>.

**Figure 12:** Average droplet enlargement with sawtooth DC fields at varying frequency and field intensity: (a) 67, (b) 134 and (c) 335 kV m<sup>-1</sup>. Comparison with constant DC fields.

**Figure 13:** Probability density functions of inlet and outlet water droplet size distributions under half-sinusoidal DC fields at varying frequency and field intensity: (a) 67, (b) 134 and (c) 335 kV m<sup>-1</sup>.

**Figure 14:** Average droplet enlargement with half-sinusoidal DC fields at varying frequency and field intensity: (a) 67, (b) 134 and (c) 335 kV m<sup>-1</sup>. Comparison with constant DC fields.

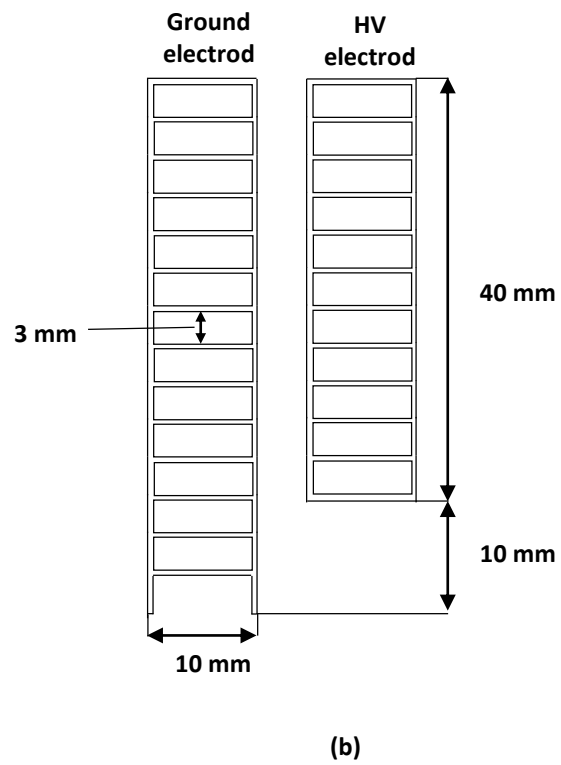
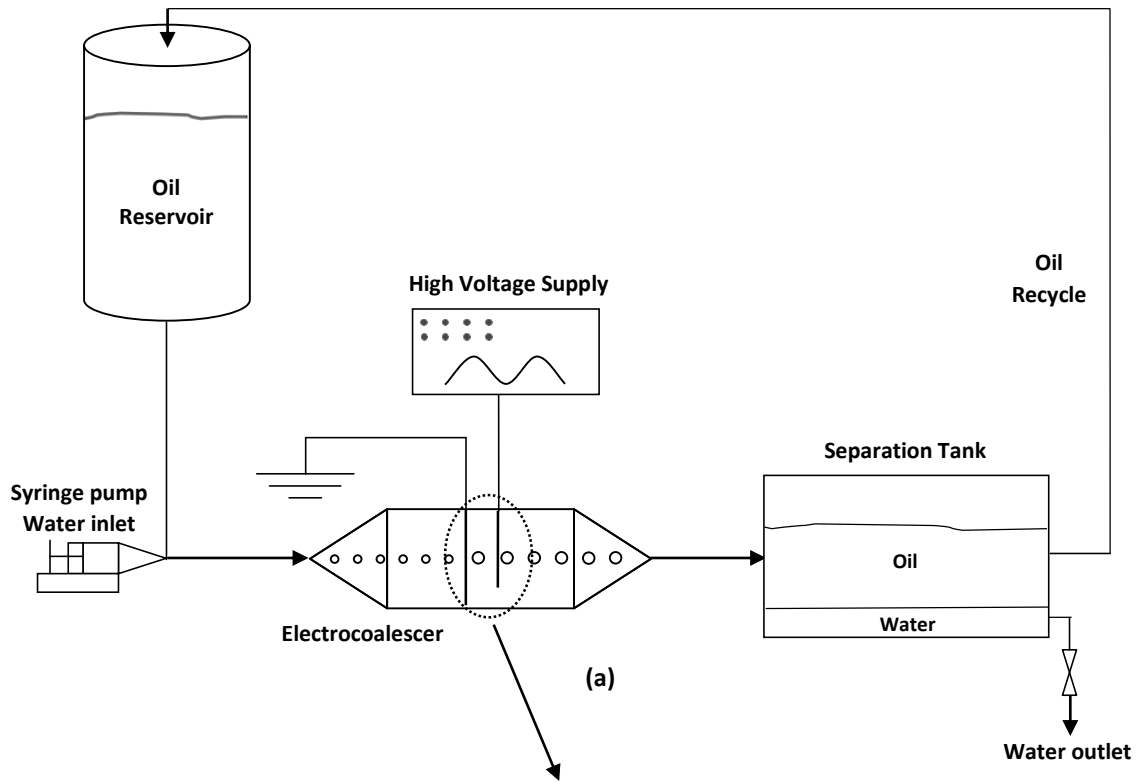
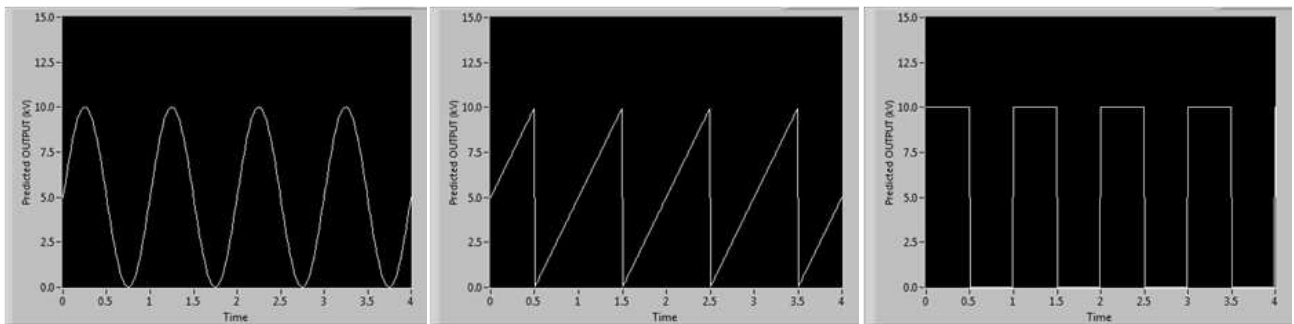


**Figure 1.** Experimental rig and electrode design.



(a)

(b)

(c)

**Figure 2.** Waveforms generated by the high voltage unit: (a) sinusoidal waves, (b) sawtooth waves, (c) square waves.

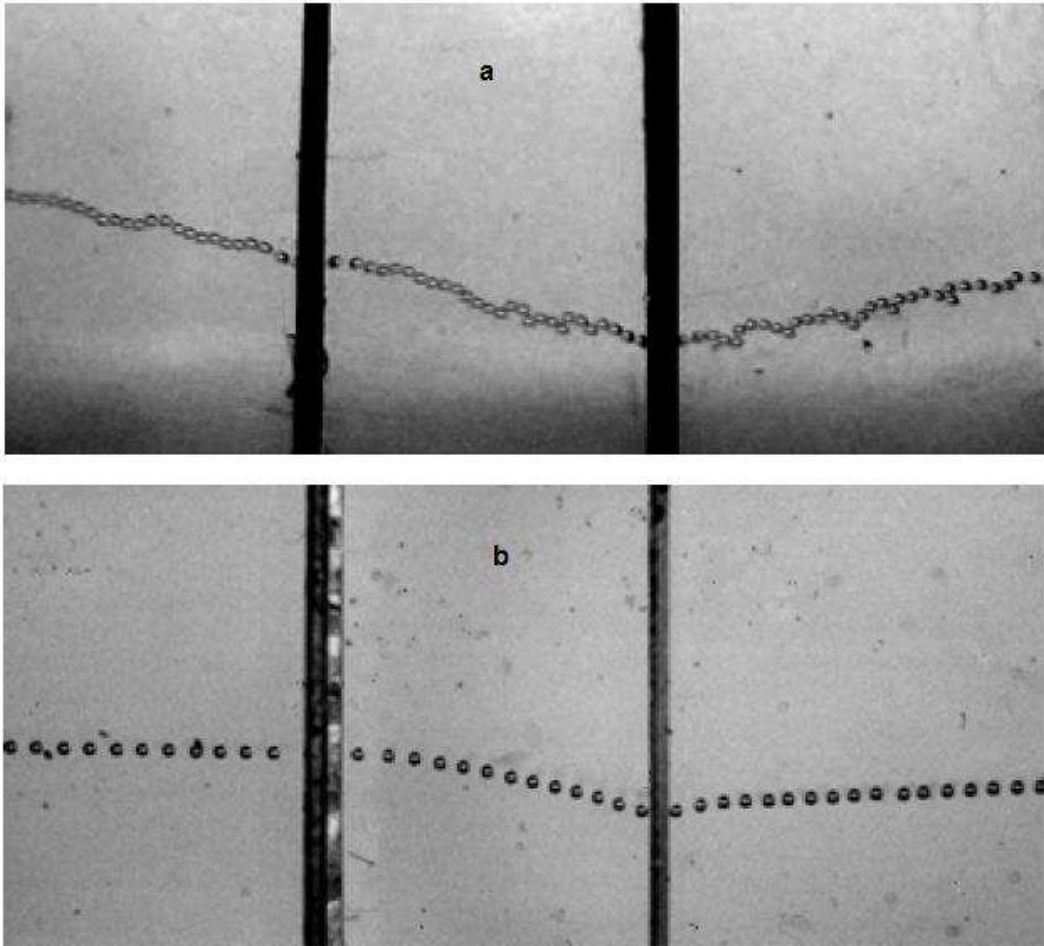


**Figure 3.** Snapshots of the droplet train for the two experimental cases:  
(a) contiguous and (b) separated droplets.

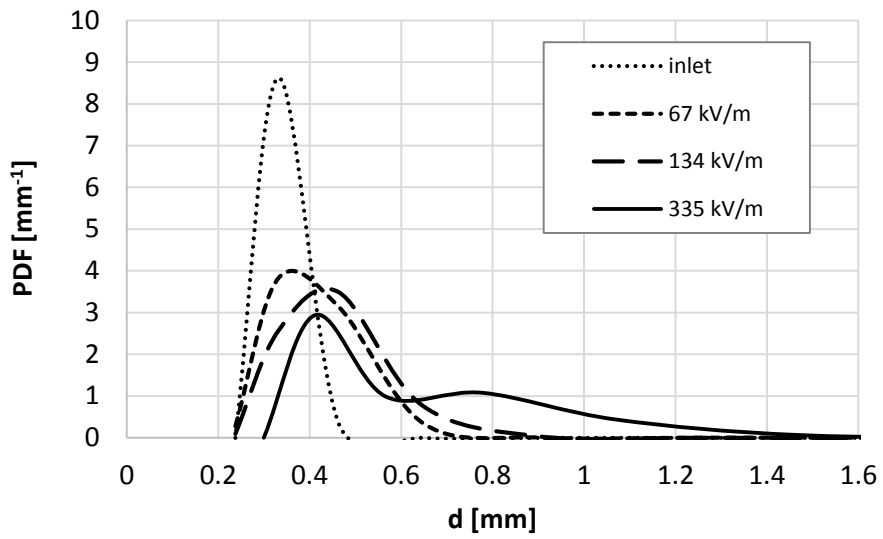


**Figure 4.** Probability density functions of water droplets size distributions under constant DC fields at varying field intensity.

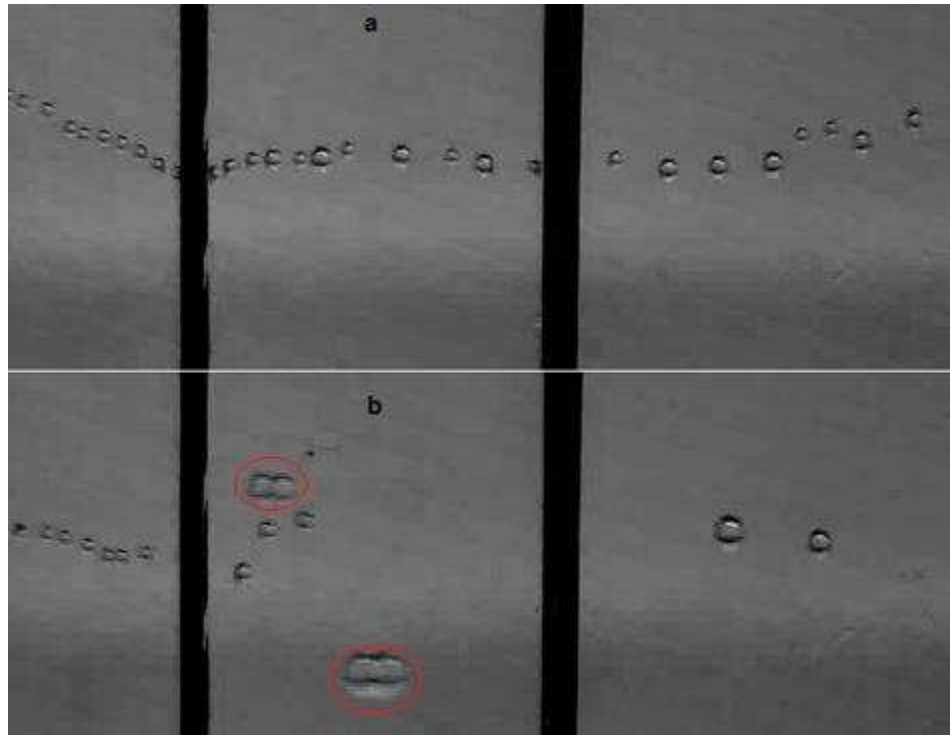


**Figure 5.** Experimental images revealing different coalescence mechanisms under constant DC fields at: a) 134 and b) 335 kV m-1.

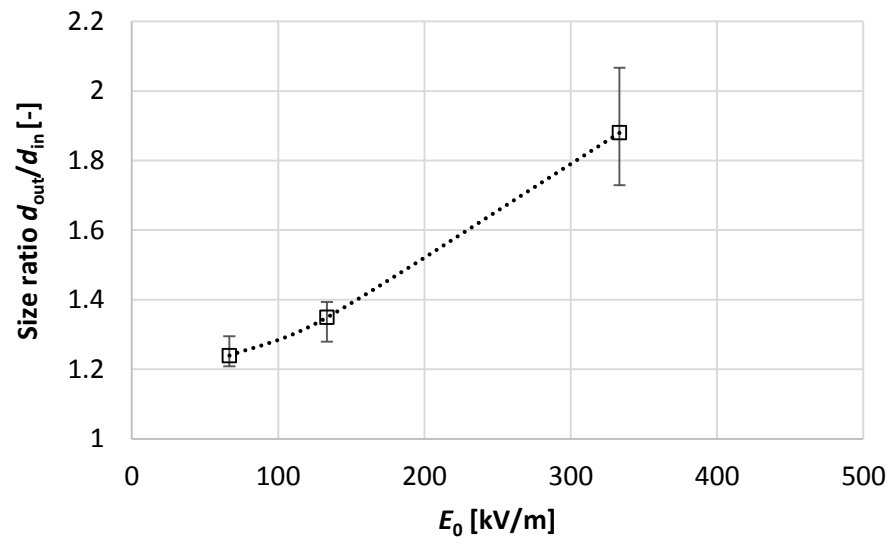


**Figure 6.** Average droplet enlargement of a train of contiguous droplets under constant electric fields.

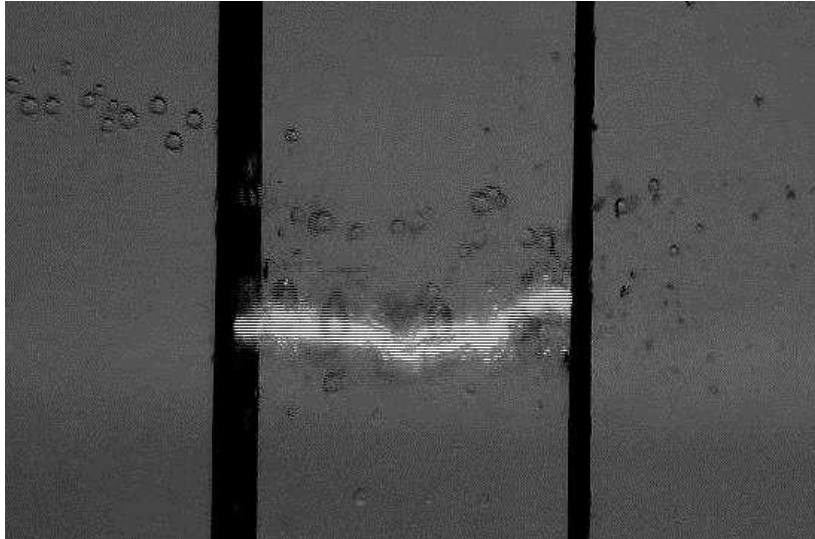


**Figure 7.** Electric discharge due to short-circuiting under a constant electric field of  $467 \text{ kV m}^{-1}$ .

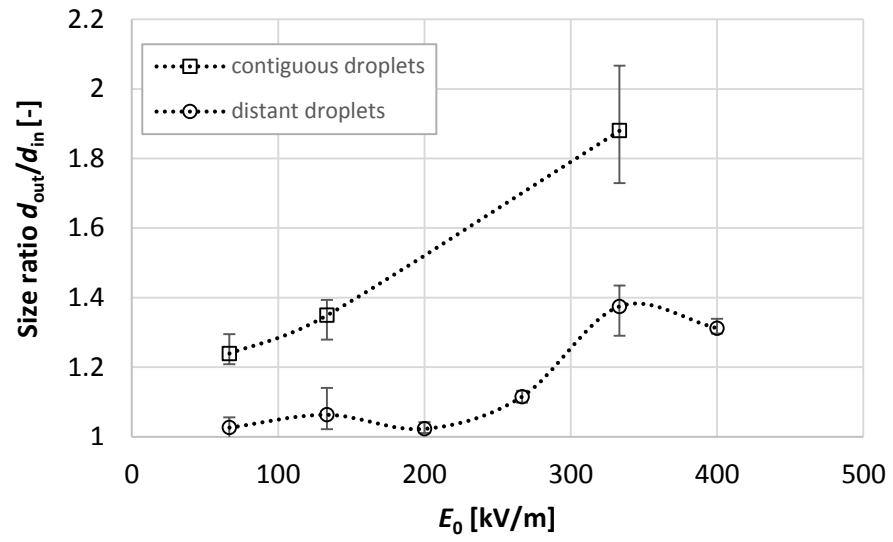
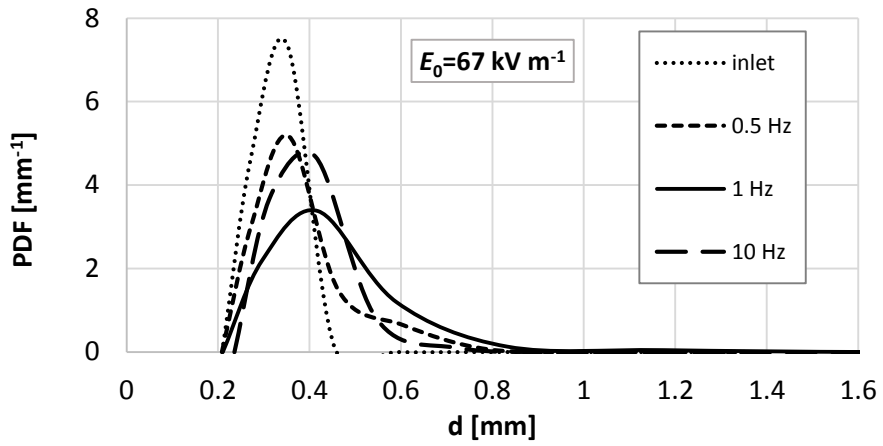
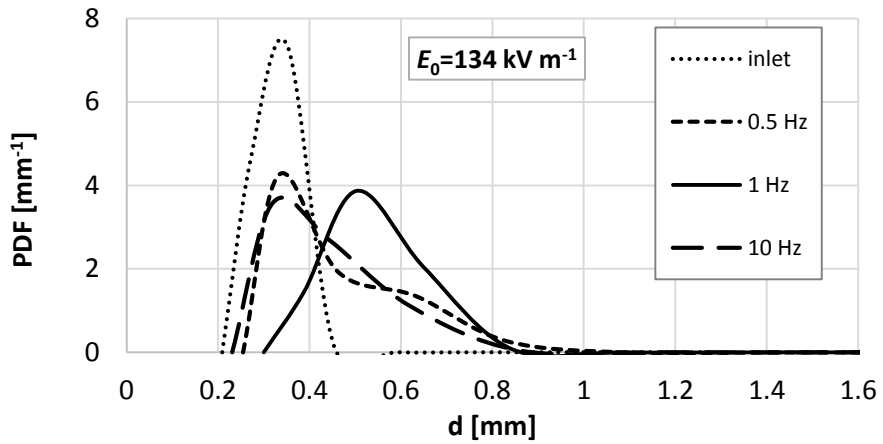


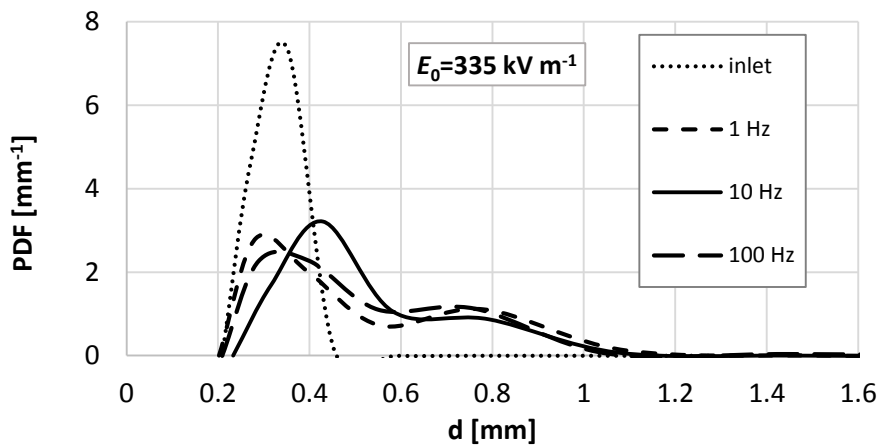
**Figure 8.** Effect of inter-droplet separation on droplet coalescence under constant electric fields.



(a)

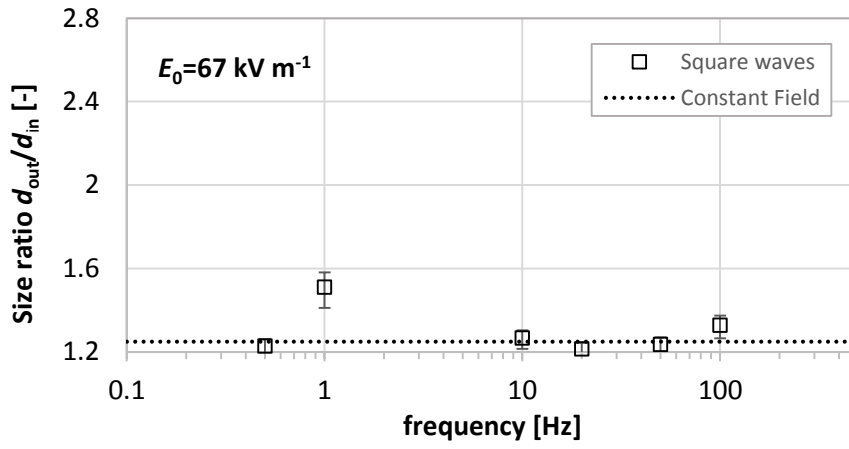


(b)

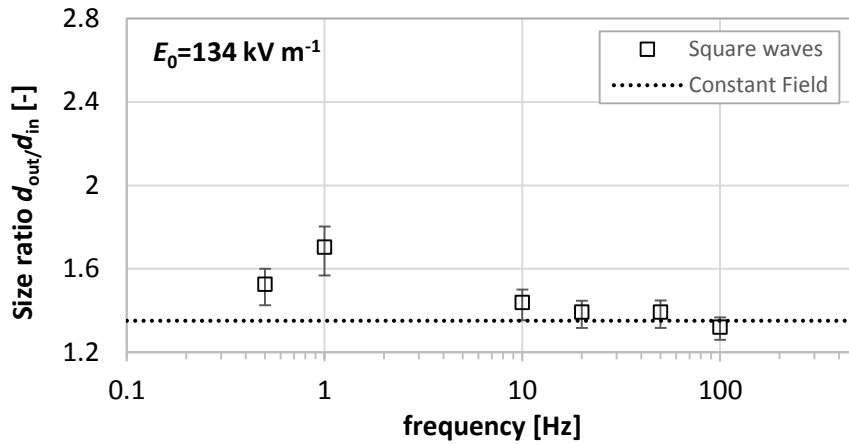


(c)

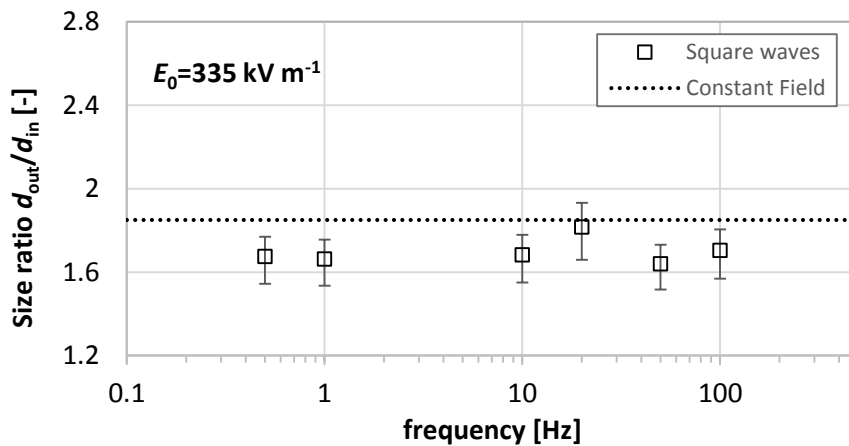
**Figure 9.** Probability density functions of inlet and outlet droplet size distributions under square DC fields at varying frequency and field intensity: (a) 67, (b) 134 and (c) 335  $\text{kV m}^{-1}$ .



(a)

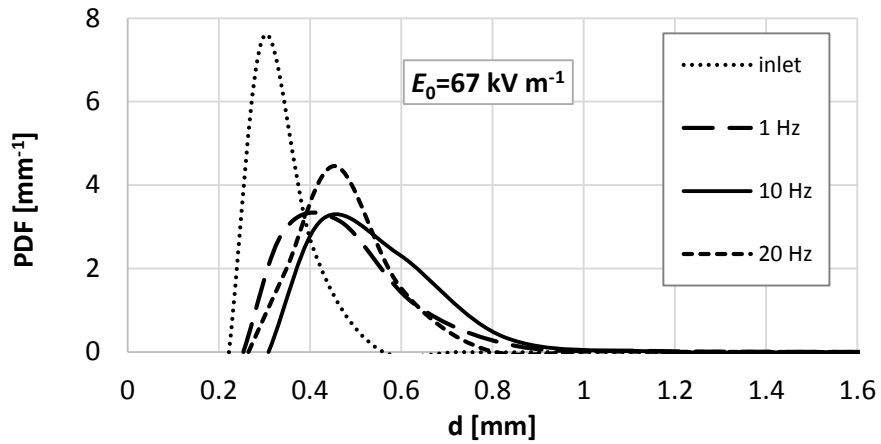


(b)

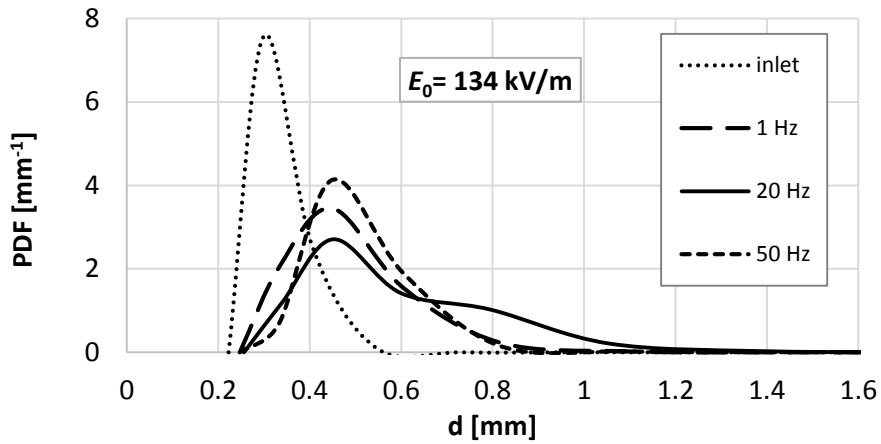


(c)

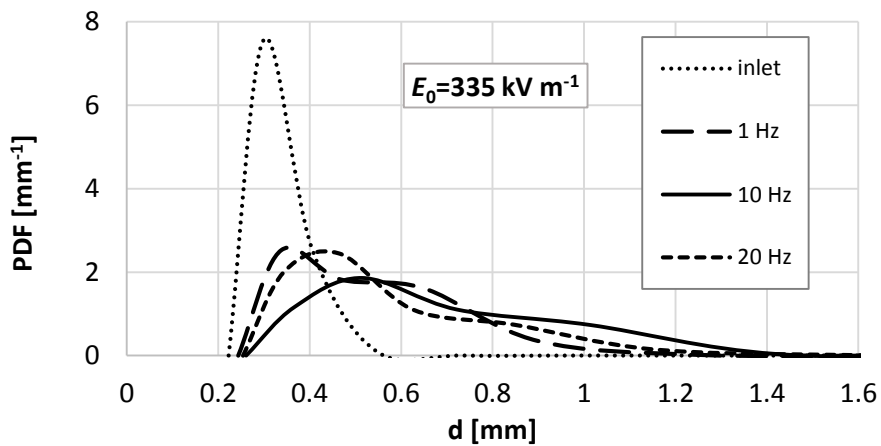
**Figure 10.** Average droplet enlargement with square DC fields at varying frequency and field intensity: (a) 67, (b) 134 and (c) 335  $\text{kV m}^{-1}$ . Comparison with constant DC fields.



(a)

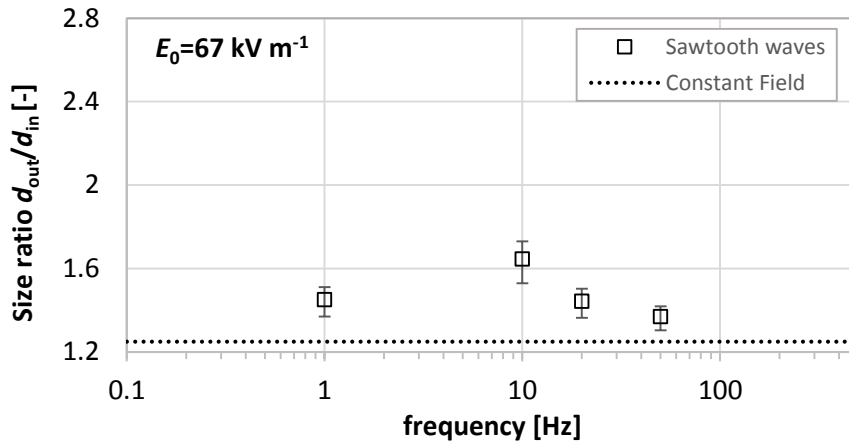


(b)

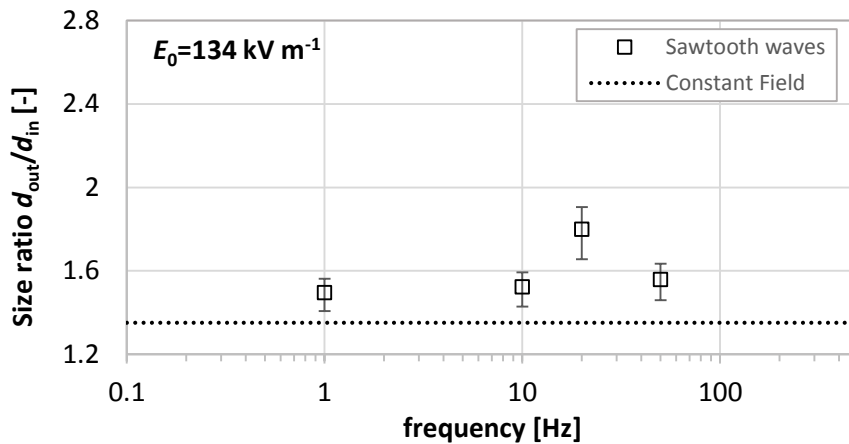


(c)

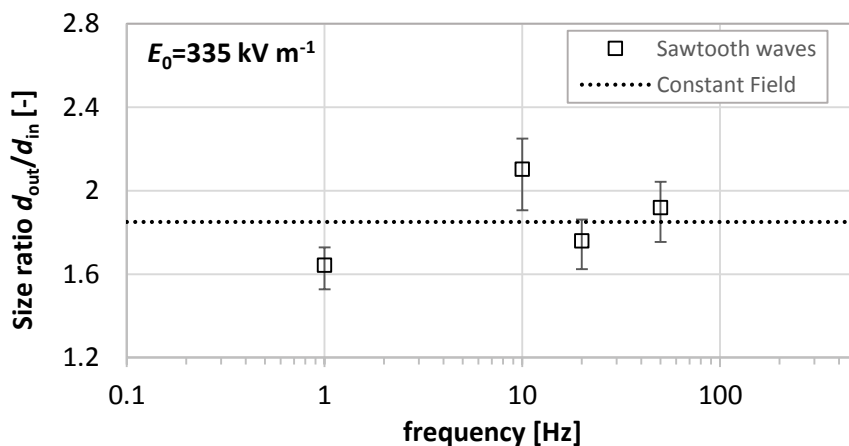
**Figure 11.** Probability density functions of inlet and outlet water droplet size distributions under sawtooth DC fields at varying frequency and field intensity: (a) 67, (b) 134 and (c) 335  $\text{kV m}^{-1}$ .



(a)

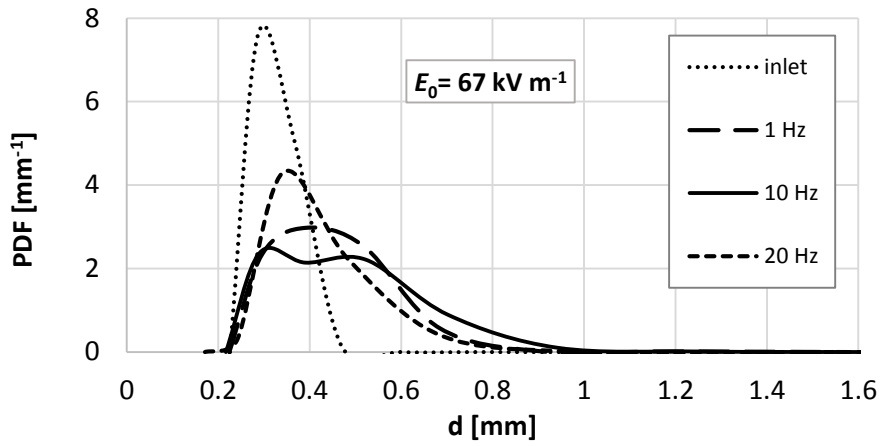


(b)

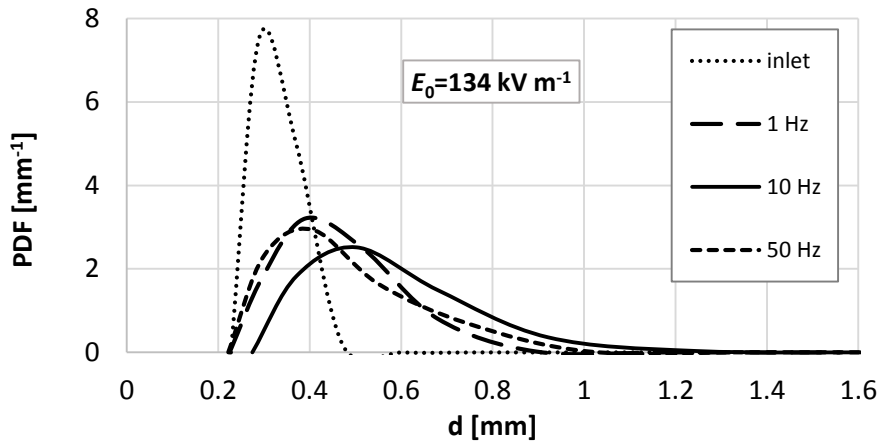


(c)

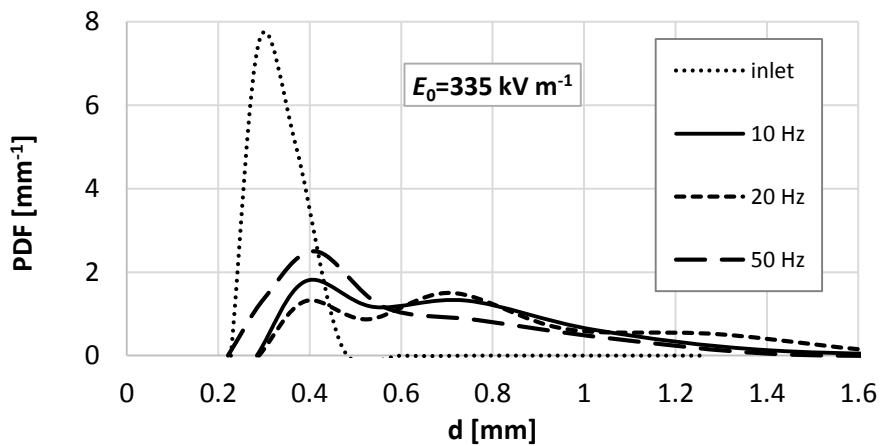
**Figure 12.** Average droplet enlargement with sawtooth DC fields at varying frequency and field intensity: (a) 67, (b) 134 and (c) 335  $\text{kV m}^{-1}$ . Comparison with constant DC fields.



(a)

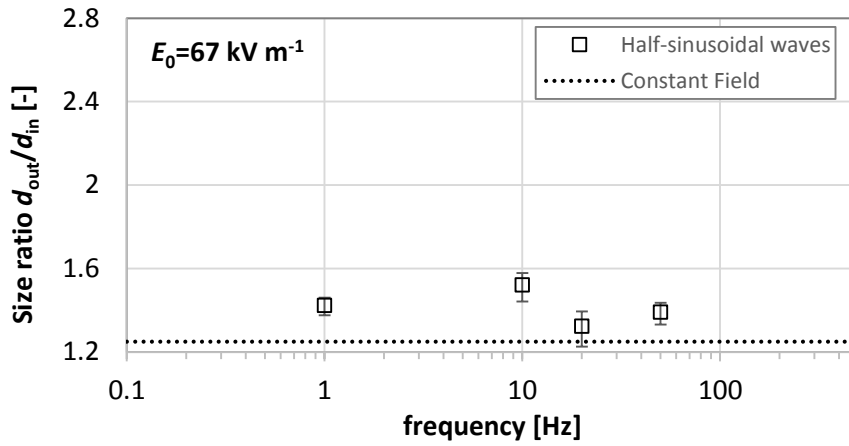


(b)

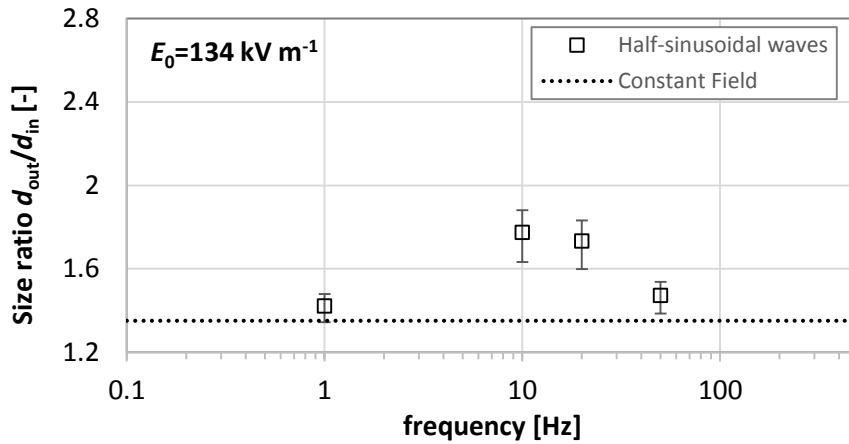


(c)

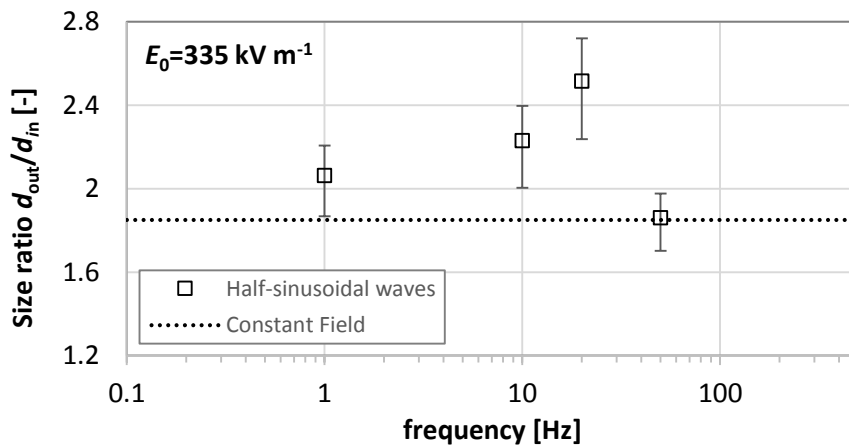
**Figure 13.** Probability density functions of inlet and outlet water droplet size distributions under half-sinusoidal DC fields at varying frequency and field intensity: (a) 67, (b) 134 and (c) 335  $\text{kV m}^{-1}$ .



(a)



(b)



(c)

**Figure 14.** Average droplet enlargement with half-sinusoidal DC fields at varying frequency and field intensity: (a) 67, (b) 134 and (c) 335  $\text{kV m}^{-1}$ . Comparison with constant DC fields.

**Table 1:** Properties of the experimental liquids.

Liquid	Conductivity $\mu\text{S m}^{-1} (\pm 5\%)$	Viscosity mPa s	Interfacial tension $\text{mN m}^{-1}$	Density $\text{kg m}^{-3}$	Dielectric constant -
Tap-water	$4.1 \times 10^4$	1.00	73	998	80
Sunflower oil	$3.6 \times 10^{-6}$	46.5	33	920	4.9

**Table 2.** Theoretical RMS and average values of the field for the different waveforms used.

Waveform	RMS	Average
Square	$E_0 \frac{\sqrt{2}}{2}$	$\frac{E_0}{2}$
Sawtooth	$E_0 \frac{\sqrt{3}}{3}$	$\frac{E_0}{2}$
Half-sinusoidal	$E_0 \frac{\sqrt{2}}{2}$	$E_0 \frac{2}{\pi}$